Dalton Transactions

COMMUNICATION

View Article Online
View Journal | View Issue

Cite this: *Dalton Trans.*, 2015, **44**, 14589

Received 13th May 2015,
Accepted 17th July 2015

DOI: 10.1039/c5dt01801c

www.rsc.org/dalton

Aggregation induced phosphorescent *N*-oxyde-2,2′-bipyridine bismuth complexes and polymorphism-dependent emission†

Oksana Toma,[a] Nicolas Mercier,*[a] Magali Allain,[a] Alessandra Forni,*[b] Francesco Meinardi[c] and Chiara Botta*[d]

Unprecedented bismuth complexes, based on the rarely used ditopic ligand *N*-oxide-2,2′-bipyridine (bp2mo), crystallizing as three polymorphs, α- (1), β- (2) and γ-[$BiBr_3$(bp2mo)$_2$] (3), exhibit phosphorescence with a quantum yield up to 17% for the crystal phase (1), while the complex displays a weak fluorescence in solution. A study of the luminescence properties combined with DFT/TDDFT calculations reveals that the lighting phenomenon originated by aggregation induced phosphorescence correlated with the weak intermolecular interactions present in the different crystal phases.

While most of the luminogens undergo a reduction of the emission properties upon aggregation (concentration quenching), some compounds, while non-emissive in solution, become emissive in the solid state. These phenomena are often described as aggregation induced emission (AIE)[1] and, in particular, crystallization induced emission if the emission enhancement occurs only in the crystal and not in the amorphous state.[1b] Since most of the applications in optoelectronics require solid state materials, the interest in compounds showing AIE has shown a very rapid increase. In particular the search for organometallic complexes showing enhanced phosphorescence efficiency in the aggregated state is of great interest. Li and co-workers discovered the aggregation-induced phosphorescence (AIP) phenomenon for the first time in iridium(III) complexes.[2] Thanks to the work of Tang and coworkers the AIE and AIP processes have been rationalized generally in terms of restriction of intramolecular motion (RIM) in aggregated states, which blocks the rotations and vibrations responsible for the non-radiative pathways in non-rigid environments.[3] To date, organometallic complexes with AIP properties have been reported for several metals, including Ir, Zn, Pd, Pb, Os, Re, and Pt.[4] The interest in such materials arises from their possible use in several fields. For example, the assembly and disassembly process of such complexes, able to induce a color change or to switch the emission on and off, can be a powerful tool to obtain dynamic labels for biomedical applications.[5] Indeed, the two often concomitant and opposite effects of concentration quenching and restriction of intramolecular motion make it quite difficult to fully control the relationships between structural and emissive properties in these systems.[6] The availability of different polymorphs of a well characterized phosphorescent complex provides the best opportunity to study the relationship between crystal packing and emissive properties.[4f,7]

The oxidized 2,2′-bipyridine derivatives that are *N*-oxide-2,2′-bipyridine (bp2mo) and *N*,*N*′-dioxide-2,2′-bipyridine (bp2do) have been by far less explored than the oxidized 4,4′-bipyridine ligands (*N*-oxide-4,4′-bipyridine (bp4mo) and *N*,*N*′-dioxide-4,4′-bipyridine (bp4do))[8–10] in coordination chemistry. To the best of our knowledge, no bismuth complex or coordination polymer based on bp2mo has been reported until now, nor based on bp2do, bp4mo or bp4do. Moreover, we can also note that complexes with N atoms coordinated to Bi^{3+} are not so common. For instance, according to the Cambridge Structural Database[11] only a few structures of Bi-bp4 complexes are known (bp4:4,4′-bipyridine). Nevertheless, we have recently shown that bipyridine derivatives consisting of one pyridinium cycle (acting as an electron acceptor) and one pyridyl (*N*-methyl-4,4′-bipyridinium) or one pyridyl-*N*-oxide part (*N*-R-*N*′-oxide-4,4′-bipyridinium (R = methyl, H)) were able to bind bismuth ions.[12] In this work, we report on three polymorphic complexes in the $BiBr_3$/bp2mo system: α- (**1**), β- (**2**) and γ-[$BiBr_3$(bp2mo)$_2$] (**3**). A study of the luminescence properties

[a]*MOLTECH-Anjou UMR-CNRS 6200, 2 Bd Lavoisier, 49045 Angers, France. E-mail: nicolas.mercier@univ-angers.fr; Fax: +33 (2) 41 73 5405; Tel: +33 (2) 41 73 5083*

[b]*Istituto di Scienze e Tecnologie Molecolari – Consiglio Nazionale delle Ricerche (ISTM-CNR), Università degli Studi di Milano, via C. Golgi 19, 20133 Milano, Italy. E-mail: a.forni@istm.cnr.it*

[c]*Dipartimento di Scienza dei Materiali, Università degli Studi di Milano Bicocca, via Cozzi 55, I-20125 Milano, Italy*

[d]*Istituto per lo Studio delle Macromolecole (ISMAC), CNR, Via Bassini 15, 20133 Milano, Italy. E-mail: c.botta@ismac.cnr.it*

†Electronic supplementary information (ESI) available: Tables of crystal data, X-ray crystallographic files in CIF format and XRPD patterns for **1–3**, UV-Vis and PL spectra, PL decays, and details of computational results. CCDC 1062361 1062364 1062365. For ESI and crystallographic data in CIF or other electronic format see DOI: 10.1039/c5dt01801c

combined with DFT and time dependent DFT calculations and the analysis of the crystal structures show that the phosphorescence in these materials is very sensitive to the environment rigidity, being completely quenched in the solution where only a weak fluorescence signal is detected. We show that the different phosphorescence efficiencies of the three crystal phases are correlated with different non-radiative decay channels induced by their different weak intermolecular interactions.

All three phases α-(**1**), β-(**2**), and γ-[$BiBr_3$(bp2mo)$_2$] (**3**) were synthesized by a solvothermal method from a mixture of $BiBr_3$ and bp2mo with acetonitrile as the solvent. Slight differences in the stoichiometry of reagents as well as in the temperature program have led to obtaining each of the three compounds as pure phases, as checked by the XRPD diffraction method (see the ESI†). The X-ray single crystal structures of **1–3** have been refined in the space groups of $P\bar{1}$, $P2_1/n$ and $P2_1/c$, respectively.‡ In all the three structures of **1–3**, a similar neutral complex based on one bismuth ion surrounded by 3 bromides and two bp2mo molecules is found. The geometrical characteristics associated with all these complexes (3 independent complexes in the structure of α, named **1a**, **1b** and **1c** in the following, and only 1 in the structures of β and γ) are somewhat different, particularly the dihedral angles between the two cycles of bp2mo molecules and the Bi–N or Bi–O bond distances as well. The two bp2mo molecules are connected to Bi^{3+} *via* their pyridyl and pyridyl-*N*-oxide part. The dihedral angle between the two rings (30°–46° range) results from both the N–Bi bond, Bi being in the plane defined by the pyridyl ring, and the (N)O–Bi coordination which involves a N–O–Bi bond angle close to 120° (Fig. 1a). The resulting complex which is completed by three bromides is chiral. But it must be noted that the two chiral forms are present in **1–3** on account of the centrosymmetrical nature of their crystal structure. The overall structures of the three polymorphs differ by the packing of these complex units (the structure of **1** is given in Fig. 1b, and those of **2** and **3** are given in the ESI, Fig. S2 and S3†). The more densely packed is that of α (**1**) since the unit cell volume is smaller ($2/3V_\alpha$ = 2266 Å^3), then β (**2**) (V_β = 2313 Å^3) and finally γ (**3**) (V_γ = 2367 Å^3). The crystal structure analysis also shows that potential transformations of one phase to another seem difficult.

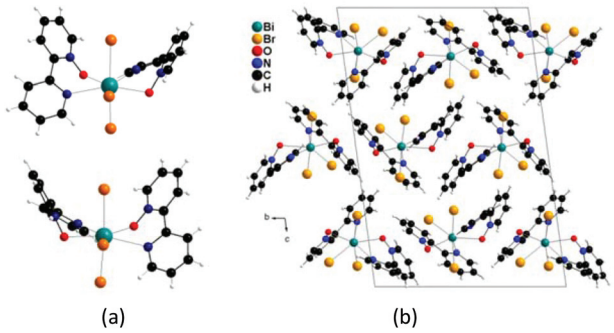

Fig. 1 (a) The two chiral forms of bismuth complexes found in the structures of α-, β- and γ-[$BiBr_3$(bp2mo)$_2$] (**1–3**); (b) crystal structure of **1** viewed along *a*.

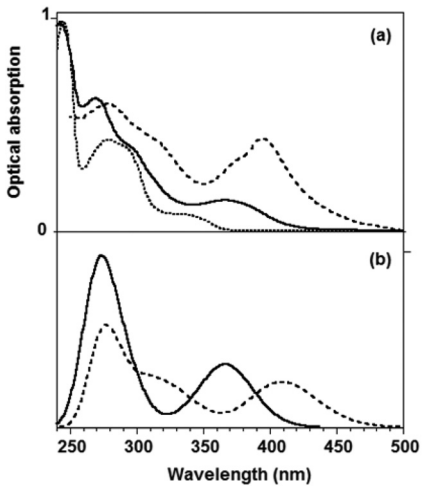

Fig. 2 (a) Experimental absorption spectra of bp2mo solution (dotted line), [$BiBr_3$(bp2mo)$_2$] solution (solid line) and α-[$BiBr_3$(bp2mo)$_2$] (**1**) solid state (dashed line). (b) Calculated absorption spectrum of [$BiBr_3$(bp2mo)$_2$] in solution (solid line) and of polymorph **1** (dashed line), obtained by averaging the spectra of **1a**, **1b** and **1c**, resulting from convolution of the excitation energies with 0.2 eV of half-bandwidth.

The experimental absorption spectra of [$BiBr_3$(bp2mo)$_2$] and the ligand in solution are reported in Fig. 2 together with the calculated absorption spectrum of the complex. The lower energy absorption peak of the complex (367 nm) is red-shifted with respect to the ligand (335 nm). Theoretical calculations on the optimized geometries of both the ligand and complex allowed us to well reproduce the absorption peaks observed in solution. In particular, TD-PBE0/6-311++G(d,p) calculations on the ligand predicted the lowest transition at 324 nm with an oscillator strength f = 0.026, while TD-M062X/def2-SVP calculations on the complex provided the lowest absorption at 369 nm with f = 0.057. This absorption band is principally due to the HOMO → LUMO transition, where HOMO is localized essentially on the inorganic part of the complex and LUMO on the organic ligands (see Fig. 3). It is worth noting that such a transition, while associated with a significant charge redistribution within the complex, does not imply charge transfer along a specific direction because the dipole moment is essen-

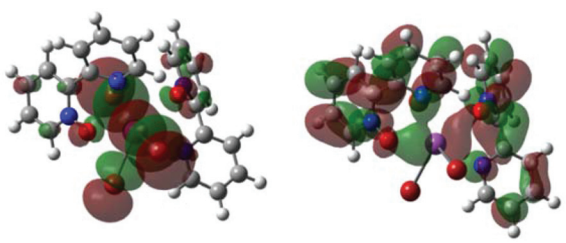

Fig. 3 Plots of M062X/def2-SVP HOMO (left) and LUMO (right) of the optimized geometry of [$BiBr_3$(bp2mo)$_2$] with an isosurface value of 0.02.

tially unchanged from the ground (9.75 D) to the excited state (8.05 D). The second peak computed for the complex at 345 nm (f = 0.015, hidden in the convoluted spectrum, see excitation energies in Fig. S11a†) corresponds principally to the HOMO → LUMO+1 transition, where LUMO+1 is well localized on the ligands, while the large body of transitions giving the maximum at 274 nm (observed in solution at 270 nm with a shoulder at 295 nm) involve essentially orbitals localized on ligands or bromine atoms.

The three polymorphs give rise to essentially the same absorption spectrum (Fig. S7†), where the absorption maximum (395, 396 and 392 nm for **1**, **2** and **3**, respectively) is red-shifted with respect to the solution phase (see Fig. 2(a)). TDDFT calculations on the X-ray experimental geometries of **1–3** reproduced as well the red-shift of the absorption maxima with respect to the values obtained at the optimized geometries, with λ_{max} peaked at 410, 414 and 400 nm for the three molecules of the asymmetrical unit of **1**, and at 390 and 410 nm for **2** and **3**, respectively (see Fig. 2b, Fig. S11b–f and Table S2†). The two polymorphs **1** and **3** show bright greenish-yellow emissions in the solid state (see Fig. 4, Fig. S7, and S8, and Table S1†), characterized by different PL efficiencies and lifetimes indicative of emission from a triplet state (QY = 17%, τ = 4.8 μs, Commission International d'Eclairage CIE (1931) of (0.34;0.61), λ_{max} 525 nm for **1**; QY = 5%, τ = 1.0 μs, λ_{max} 503 nm for **3**). Polymorph **2** displays a very weak (λ_{max} 516 nm QY *ca.* 0.5%) broad emission. On the other hand, the complex $[BiBr_3(bp2mo)_2]$ displays an extremely weak emission in solution (QY = 0.01%) with a PL spectrum peaked in the blue region (about 442 nm) characterized by a very short lifetime (258 ps) (see Fig. S9 and S10†). The different lifetimes and energy positions of the emission in the solid state with respect to the solution suggest its origin from a triplet excited state for the former case, and from a singlet excited state for the latter.

To gain insight into the nature of the emissive states of the investigated complex, the computed lower energy singlet (S_1) and triplet (T_1) excited states were subjected to geometry optimization. The obtained stationary states of S_1 and T_1 were quite similar in geometry and the computed emission energies were 669 and 778 nm, respectively. Emission from S_1 could be reasonably associated with the emission peak observed in solution, though placed at a lower energy with respect to the experimental one. The observed discrepancy should be ascribed to the intrinsic limitations of the theoretical approach in accurately locating the emissive states when heavy atoms such as bismuth are present. From analysis of the optimized geometries of S_1 and T_1, it results that one bp2mo ligand of the complex underwent a partial planarization with respect to the ground state S_0 geometry (the NCCN torsion angle changes from 44 to 23° and 26° in S_1 and T_1, respectively), while the other ligand essentially preserves its distortion (the NCCN torsion angle changes from 50 to 47° in both S_1 and T_1). The 'planarized' ligand acquires a pseudo-quinoid structure where both the Bi–O and Bi–N bonds significantly strengthen with respect to the S_0 minimum energy geometry (bond lengths go from 2.438, 2.714 in S_0 to 2.237, 2.471 and 2.334, 2.474 Å in S_1 and T_1, respectively). The $S_1 \rightarrow S_0$ transition is characterized by an oscillator strength f = 0.008 quite lower than the $S_0 \rightarrow S_1$ one.[13] This finding, coupled with the detected quite fast PL decay time, demonstrates the presence of fast non-radiative decay channels determining the weak PL intensity observed in solution. It is to be noted that at both S_1 and T_1 optimized geometries, the LUMO is localized only on the more planar ligand, while the HOMO essentially preserves its distribution on the inorganic part of the complex (see Fig. S12†). Planarization of the ligand, as obtained in the optimized excited states, suggests that the observed emission in the solid state is induced by restriction of the torsional motion around the bond connecting the two pyridine moieties.

In order to verify the AIP origin of the emission of the complex in the solid state, we measured the emission of THF frozen solutions of $[BiBr_3(bp2mo)_2]$ (see Fig. 4). Upon solvent solidification the weak blue emission turns into bright greenish-yellow (530 nm), being very similar to the solid state one but showing a broader spectral shape, with CIE of (0.39;0.55) (see photos in Fig. S13†). By heating the frozen solution, only a reduction in the intensity is observed until the melting point of the solvent is reached. Above this temperature the greenish-yellow emission is completely quenched and only weak deep blue emission, with CIE of (0.15;0.12), is observed (see the inset of Fig. 4). Since the sharp quenching of the solution emission occurs exactly at the melting point of the solvent, we assign it to the loss of rigidity of the environment that allows the mobility of the complex ligands. In contrast, by rigidification of the solvent matrix of a ligand solution, only minor changes in the emission properties are observed (see Fig. S9†). These results demonstrate that the bright phosphorescence emission of the complex crystals can be assigned to their rigidity that prevents intramolecular motion of the ligands. The broadening of the emission band with respect to that observed for **1** and **3** should be ascribed to the amorphous nature of the frozen solution. The different nature of the emissive states

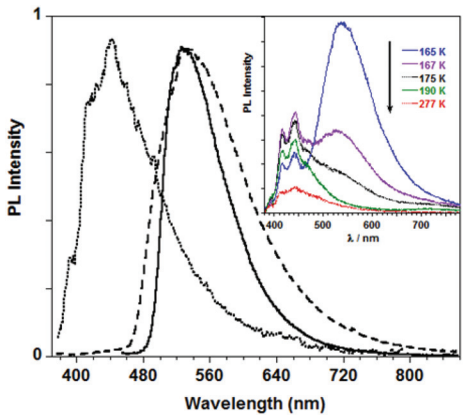

Fig. 4 Normalized PL spectra of $[BiBr_3(bp2mo)_2]$ THF solutions at room temperature (dotted line) and at 82 K (dashed line). The PL spectrum of polymorph **1** at room temperature (solid line). Insert: PL spectra of the solution at different temperatures.

(triplet *vs.* singlet) in the rigid environment (solid state and frozen solution) with respect to the solution suggests that the presence of a heavy atom such as Bi induces a fast decay of S_1 *via* intersystem crossing to the low-lying T_1 triplet. However, the long living phosphorescence of the latter is completely quenched in solution by free intramolecular motion, while the short lived singlet state still preserves in any case a weak fluorescence.

Since emission in the solid state originates principally from only the T_1 excited state, the stronger emission of polymorph **1** with respect to **2** and, to a lesser extent, **3** should be ascribed to a more efficient inhibition of the non-radiative processes connected to intramolecular rotation of the ligands and vibrational relaxation processes. In other words, polymorph **1** seems to possess a higher RIM (Restriction of Intramolecular Motions) property. This interpretation is also confirmed by the observation of the weak emission of films obtained by solution casting. Indeed, as already reported for both organic molecules and complexes, in some cases AIE is not efficient in amorphous films and emission enhancement occurs only in the crystal phase.[3,14,15b] The comparison of these three different crystal polymorphs evidences the important role of crystal packing in phosphorescent complexes that show crystallization induced phosphorescence. In particular, the different non-radiative decay rates of **1** and **3** (see Table S1†) suggest that the greater QY of **1** is ascribed to its lower rate of non-radiative decay from T_1. According to previous studies,[15] the non-radiative relaxation can be reduced by the presence of weak intermolecular interactions in the solid state, unlike stronger interactions such as π–π stacking which would favour the formation of detrimental excimers. By analyzing the intermolecular interaction network in the crystal structures of **1–3**, we note that only in **1** weak π–π interactions are present (see Fig. S1†), while, in all structures, several C–H···Br, C–H···O and C–H···π interactions hold the molecules in their crystalline lattice in a different way (see Table S3†). Such hydrogen bonds involve in all cases C–H bonds of one organic ligand and, for C–H···O and C–H···π interactions, an acceptor group of another organic ligand, determining an efficient reduction of their conformational flexibility and then of their non-radiative relaxation channel. Moreover, comparing the structures of **1–3**, we observe that, while C–H···Br interactions are similar in the three structures, 'stronger' C–H···O and C–H···π hydrogen bonds are found in **1** and **3**, which may explain their higher luminescence with respect to **2**. On the other hand, the higher QY of **1** with respect to **3** could be explained by the lower number of intermolecular interactions found in the latter structure.

In conclusion, we have demonstrated, for the first time for a Bi based complex, that the solid state emission of the $[BiBr_3(bp2mo)_2]$ complex has an aggregation-induced phosphorescence origin due to restriction of intramolecular motion. We have shown that the phosphorescence efficiency in the solid state is different for the three crystal phases according to their different weak intermolecular interactions. This study highlights the role of even weak intermolecular interactions in the photophysical properties of materials whose phosphorescence originated by restriction of intramolecular motion.

A. F. acknowledges the MIUR for the PRIN 2010–2011 project no. 2010ERFKXL. C. B. thanks Regione Lombardia for funding (project "Tecnologie e materiali per l'utilizzo efficiente dell'energia solare" decreto 3667/2013). N. M. thanks the LUMOMAT regional program for a post-doc fellowship to O. T. (Bipylum project).

Notes and references

‡Crystal data for **1–3** ($C_{20}H_{16}BiBr_3N_4O_2$, M = 793.08, T = 293 K): (**1**), triclinic, a = 9.6004(4) Å, b = 15.6899(4) Å, c = 22.9678(5) Å, α = 97.53(1), β = 93.73(1)°, γ = 96.04(1)°, V = 3399.8(2) Å^3, space group $P\bar{1}$, Z = 6, crystal size (mm^3): 0.20 × 0.06 × 0.04. (**2**): monoclinic, a = 9.748(1) Å, b = 13.011(1) Å, c = 18.253(3) Å, β = 91.88(1)°, V = 2313.8(5) Å^3, $P2_1/n$, Z = 4, crystal size (mm^3): 0.11 × 0.06 × 0.06. (**3**): monoclinic, a = 13.5654(1) Å, b = 9.6701(1) Å, c = 18.1116(2) Å, β = 94.96(1)°, V = 2367.0(1) Å^3, $P2_1/n$, Z = 4, crystal size (mm^3): 0.29 × 0.20 × 0.16. The refinements of positions and anisotropic thermal motion parameters of the non-H atoms, converge to $R_{(F)}$ = 0.029 (2471 reflections (11 081 collected (R(int) = 0.035)), 811 parameters), w$R_{2(F2)}$ = 0.099 (all data), GOF on F^2 is 1.17, $\Delta\rho_{max}$ = 1.17 e Å^{-3} for **1**; $R_{(F)}$ = 0.071 (5867 reflections (25 911 collected (R(int) = 0.010)), 271 parameters), w$R_{2(F2)}$ = 0.245 (all data), GOF on F^2 is 1.02, $\Delta\rho_{max}$ = 1.403 e Å^{-3} for **2**, and to $R_{(F)}$ = 0.040 (4865 reflections (10 686 collected (R(int) = 0.045)), 271 parameters), w$R_{2(F2)}$ = 0.111 (all data), GOF on F^2 is 1.08, $\Delta\rho_{max}$ = 3.24 e Å^{-3} for **3**. CCDC 1062361 (**1**), 1062364 (**2**) and 1062365 (**3**).

1 (*a*) J. W. Y. Lam and B. Z. Tang, *Chem. Soc. Rev.*, 2011, **40**, 5361–5388; (*b*) Y. Dong, J. W. Y. Lam, A. Quin, Z. Li, J. Sun, H. H. Y. Sung, I. D. Williams and B. Z. Tang, *Chem. Commun.*, 2007, 40.

2 (*a*) Q. Zhao, L. Li, F. Y. Li, M. X. Yu, Z. P. Liu, T. Yi and C. H. Huang, *Chem. Commun.*, 2008, 685; (*b*) K. W. Huang, H. Z. Wu, M. Shi, F. Y. Li, T. Yi and C. H. Huang, *Chem. Commun.*, 2009, 1243.

3 J. Mei, Y. Hong, J. W. Y. Lam, A. Qin, Y. Tang and B. Z. Tang, *Adv. Mater.*, 2014, **26**, 5429–5479.

4 (*a*) G. Li, Y. Wu, G. Shan, W. Che, D. Zhu, B. Song, L. Yan, Z. Su and M. R. Bryce, *Chem. Commun.*, 2014, **50**, 6977; (*b*) J. Wang, J. Mei, R. Hu, J. Z. Sun, A. Qin and B. Z. Tang, *J. Am. Chem. Soc.*, 2012, **134**, 9956; (*c*) N. B. Shustova, T.-C. Ong, A. F. Cozzolino, V. K. Michaelis, R. G. Griffin and M. Dinc, *J. Am. Chem. Soc.*, 2012, **134**, 15061; (*d*) A. J. Qin, J. W. Y. Lam, F. Mahtab, C. K. W. Jim, L. Tang, J. Z. Sun, H. H. Y. Sung, I. D. Williams and B. Z. Tang, *Appl. Phys. Lett.*, 2009, **94**, 253308; (*e*) J. Shi, N. Chang, C. Li, J. Mei, C. Deng, X. Luo, Z. Liu, Z. Bo, Y. Q. Dong and B. Z. Tang, *Chem. Commun.*, 2012, **48**, 10675; (*f*) E. Quartapelle Procopio, M. Mauro, M. Panigati, D. Donghi, P. Mercandelli, A. Sironi, G. D'Alfonso and L. De Cola, *J. Am. Chem. Soc.*, 2010, **132**, 14397–14399; (*g*) S. Liu, H. Sun, Y. Ma, S. Ye, X. Liu, X. Zhou, X. Mou, L. Wang, Q. Zhao and W. Huang, *J. Mater. Chem.*, 2012, **22**, 22167–22173; (*h*) Y. Chen, L. Qiao, B. Yu, G. Li, C. Liu, L. Ji and H. Chao, *Chem. Commun.*, 2013, **49**, 11095; (*i*) G.-G. Shan, H.-B. Li, H.-Z. Sun, D.-X. Zhu, H.-T. Cao and Z.-M. Su, *J. Mater.*

Chem. C, 2013, **1**, 1440; (*j*) G.-G. Shan, D.-X. Zhu, H.-B. Li, P. Li, Z.-M. Su and Y. Liao, *Dalton Trans.*, 2011, **40**, 2947.

5 M. Mauro, A. Aliprandi, D. Septiadi, N. S. Kehr and L. De Cola, *Chem. Soc. Rev.*, 2014, **43**, 4144.

6 Z. Wei, Z.-Y. Gu, R. K. Arvapally, Y.-P. Chen, R. N. McDougald Jr., J. F. Ivy, A. A. Yakovenko, D. Feng, M. A. Omary and H.-C. Zhou, *J. Am. Chem. Soc.*, 2014, **136**, 8269–8276.

7 H. Unesaki, T. Kato, S. Watase, K. Matsukawa and K. Naka, *Inorg. Chem.*, 2014, **53**, 8270–8277.

8 (*a*) A.-C. Chamayou and C. Janiak, *Inorg. Chem. Acta*, 2010, **363**, 2193; (*b*) S. A. Bourne and L. J. Moitsheki, *J. Chem. Crystallogr.*, 2007, **37**, 359; (*c*) J. Jia, A. J. Blake, N. R. Champness, P. Hubberstey, C. Wilson and M. Schröder, *Inorg. Chem.*, 2008, **47**, 8652; (*d*) H. W. Roesky and M. Andruh, *Coord. Chem. Rev.*, 2003, **236**, 91–119.

9 R. J. Hill, D.-L. Long, N. R. Champness, P. Hubberstey and M. Schröder, *Acc. Chem. Res.*, 2005, **38**, 337; D.-L. Long, A. J. Blake, N. R. Champness, C. Wilson and M. Schröder, *J. Am. Chem. Soc.*, 2001, **123**, 3401; R. J. Hill, D.-L. Long, M. S. Turvey, A. J. Blake, N. R. Champness, P. Hubberstey, C. Wilson and M. Schröder, *Chem. Commun.*, 2004, 1792.

10 (*a*) D. J. Hoffart, N. C. Habermehl and S. J. Loeb, *Dalton Trans.*, 2007, 2870; (*b*) O. Toma, N. Mercier, M. Bouilland and M. Allain, *CrystEngComm*, 2012, **14**, 7844–7847.

11 F. H. Allen, *Acta Crystallogr., Sect. B: Struct. Sci.*, 2002, **58**, 380–388.

12 (*a*) O. Toma, N. Mercier and C. Botta, *Eur. J. Inorg. Chem.*, 2013, 1113–1117; (*b*) O. Toma, N. Mercier, M. Allain and C. Botta, *CrystEngComm*, 2013, **15**, 8565.

13 TDDFT calculations do not provide information on oscillator strengths for triplet–singlet transitions since spin–orbit coupling effects are not included in current TDDFT implementations.

14 (*a*) E. Cariati, V. Lanzeni, E. Tordin, R. Ugo, C. Botta, A. Giacometti Schieroni, A. Sironi and D. Pasini, *Phys. Chem. Chem. Phys.*, 2011, **13**, 18005–18014; (*b*) Y. Dong, J. W. Y. Lam, A. Qin, J. Sun, J. Liu, Z. Li, J. Sun, H. H. Y. Sung, I. D. Williams, H. S. Kwok and B. Z. Tang, *Chem. Commun.*, 2007, 3255.

15 (*a*) H. Tong, Y. Dong, Y. Hong, M. Häussler, J. W. Y. Lam, H. H.-Y. Sung, X. Yu, J. Sun, I. D. Williams, H. S. Kwok and B. Z. Tang, *J. Phys. Chem. C*, 2007, **111**, 2287–2294; (*b*) L. Qian, B. Tong, J. Shen, J. Shi, J. Zhi, Y. Dong, F. Yang, Y. Dong, J. W. Y. Lam, Y. Liu and B. Z. Tang, *J. Phys. Chem. B*, 2009, **113**, 9098–9103; (*c*) Y. Jin, Y. Xu, Y. Liu, L. Wang, H. Jiang, X. Li and D. Cao, *Dyes Pigm.*, 2011, **90**, 311–318.